ACS OMEGA

Open Access

http://pubs.acs.org/journal/acsodf

Article

Anomalous Current Steps in 3D Graphene Electrochemical Systems at Room Temperature

Chavis Srichan,* Pobporn Danvirutai, and Adisorn Tuantranont

Cite This: *ACS Omega* 2024, 9, 19591−19600

Read Online

ACCESS | Metrics & More | Article Recommendations

ABSTRACT: In this work, we report a new phenomenon in electrochemical systems whereby uniform current steps of 1 mA per 0.5 × 0.5 × 0.1 cm^3 (width × width × depth) of electrode volume occurred during the electrodeposition of gold and silver nanoparticles onto 3D microporous graphene on nickel layers (GF/Ni) at room temperature. The effect was exhibited only at specific applied electrical potentials. The experiments (magnetic interference, temperature dependence, and surface area dependence) were repeated, and the results were reproducible. Finally, we proposed classical electrochemical theory using the Butler−Volmer equation and quantum theory using the Landauer formalism to describe this new effect. Both theories could be used to explain the experimental results: temperature dependence, surface area dependence, blocking effects, and external magnetic field dependence. In addition, the stepwise current presented in this work facilitates the trapping and supplying of a large amount of electric charge via an inherent magnetic field in a sharp time step (∼1 s). A video clip of the recorded effect can be found at https://youtu.be/pPJh45w1sUQ.

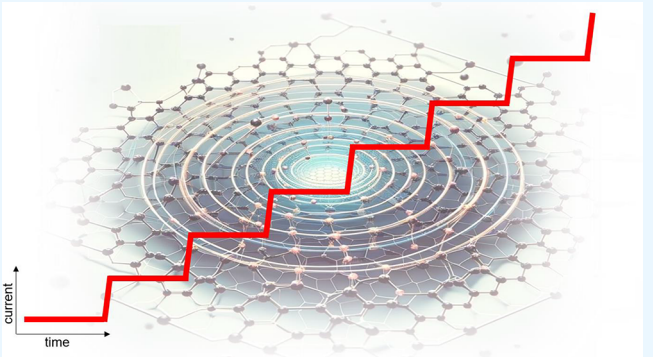

1. INTRODUCTION

Graphene has gained tremendous research attention since its discovery in 2004. Apart from zero-, one-, and two-dimensional carbon-based structures, three-dimensional graphene foam (GF) was successfully fabricated during the 2010s.[1] Afterward, wide applications of GF were reported for supercapacitors,[2] field-effect transistors,[3] electrochemical sensors,[4,5] and surface-enhanced Raman scattering (SERS) substrates.[6,7] From a theoretical point of view, the study of electronic transport in graphene-based materials could trigger ongoing progress in the physics of this two-dimensional material.[8]

Application of graphene-based materials for electrochemical sensing offers advantages such as high sensitivity, rapid response time, and accelerated electron transfer. Before we came across the stepwise current at room temperature, we planned on decorating noble metallic (gold or silver) nanoparticles on GF to be applied as SERS substrates[6,7] and highly sensitive electrodes.[4,5] At the end, we found that, for a specific active potential of approximately −0.2 V, stepwise current occurs at room temperature for both Au and Ag electrodeposition. Classical electrochemical theory and quantum theory can be applied to explanations of the experiments, including step size computation.

2. METHODS

2.1. Fabrication and Characterization. Graphene on nickel foam (GF/Ni) was prepared using chemical vapor deposition (CVD),[1] where nickel foam was used as a catalytic scaffold for CVD. C_2H_2 gas flowed to a furnace tube under 0.2 Torr at 700 °C for 3 min. Afterward, the tube underwent rapid cooling at a rate greater than 10 °C/min, and H_2 flowed at 0.1 Torr. These cause carbon atoms to form a graphene layer on the 3D foam scaffold. We electrodeposited gold into GF using $HAuCl_4{\cdot}3H_2O$ (Sigma-Aldrich) prepared in deionized water (DI) at different concentrations and applied potentials. We grew GF and cut it into 100 pieces to ensure the same conditions to determine its reproducibility, adding samples for various conditions (Figure 1). The solutions were placed over a magnetic stirrer with the speed at 400 rpm.

2.2. Electrochemical Setup. We used a three-electrode system. GF was set as the active electrode, Ag/AgCl was the reference electrode, and Pt wire was the counter electrode. By variation of the applied potential and measurement of the

Received: February 10, 2024
Revised: April 1, 2024
Accepted: April 9, 2024
Published: April 17, 2024

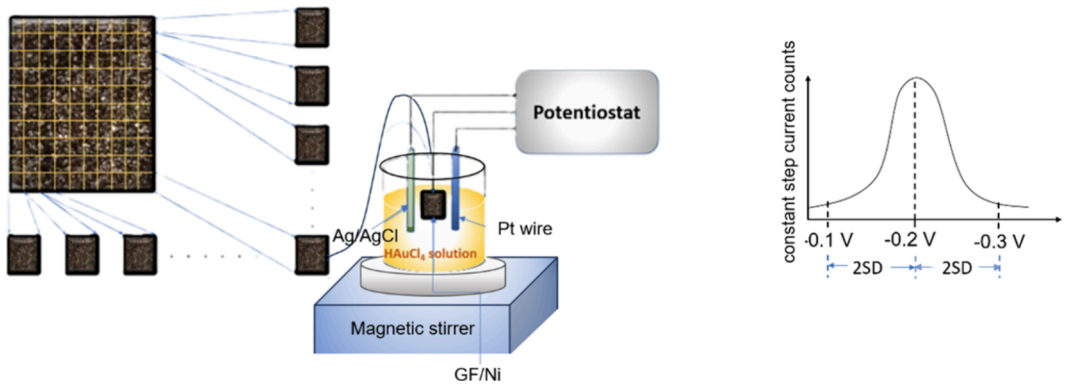

Figure 1. GF was divided into 100 equally sized pieces and used for nanoparticle growth under the same conditions. GF was placed as the working electrode. Ag/AgCl and Pt wires were used as the reference and counter electrodes, respectively. Either $HAuCl_4$ or $AgNO_3$ solutions were placed on top of the magnetic stirrer where 400 rpm speed was used. Potentials were adjusted from −0.4 to 0.0 V, and the range in which the step current could occur was recorded (−0.2 ± 0.1 V; 95% confidence).

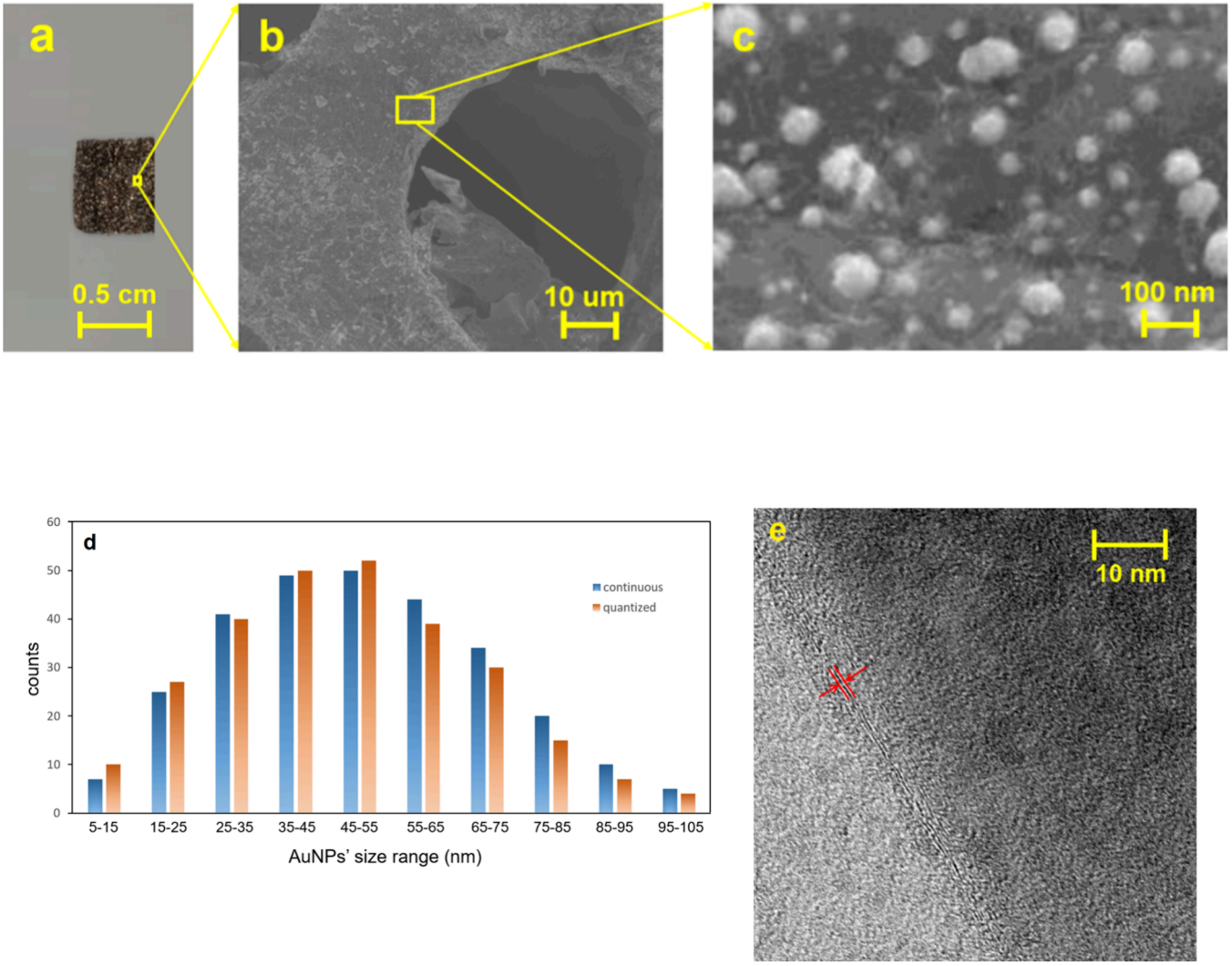

Figure 2. Characterization of the resulting AuNP/GF using (a) a camera and (b, c) a field-emission scanning electron microscope at microscale and nanoscale, respectively. The concentration of $HAuCl_4$ was 2 mM at −0.2 V potential and a 60 s deposition time. (d) AuNP's size distribution for both cases (continuous and stepwise). (e) HR-TEM illustrating the graphene layer.

amperometric current, uniform current steps were found at the applied potential of −0.2 ± 0.1 V. In other cases, the current becomes continuous. Gold ions (Au^{3+}) are supplied by gold(III) chloride trihydrate ($HAuCl_4{\cdot}3H_2O$) dissolved in DI water. While gold nanoparticles were deposited into graphene foam in amperometric mode, deposition currents were recorded over time using a potentiostat (Palmsens 2). $HAuCl_4{\cdot}3H_2O$, purchased from Sigma-Aldrich, was prepared

https://doi.org/10.1021/acsomega.4c01329
ACS Omega 2024, 9, 19591−19600

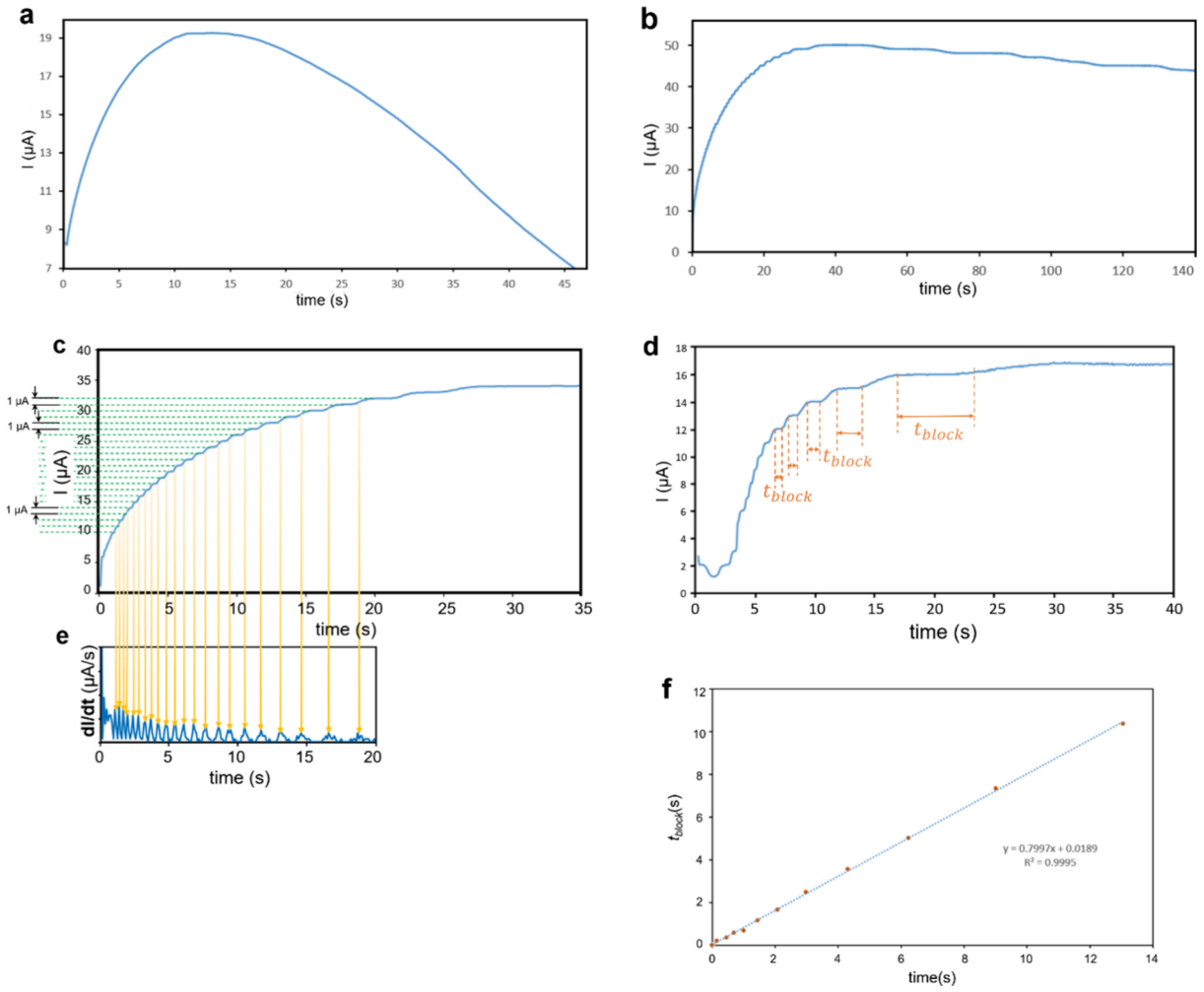

Figure 3. Electrodeposition current of Au onto GF: (a) continuous deposition current and (b–d) uniform current steps recorded. Panel (d) illustrates the blocking time denoted as t_{block}. (e) Derivative of current from panel (c) illustrating stepping positions that occurred in time series. (f) Relation of blocking time t_{block} against deposition time (s). The plot of t was offset to 0 at the starting point where current rose.

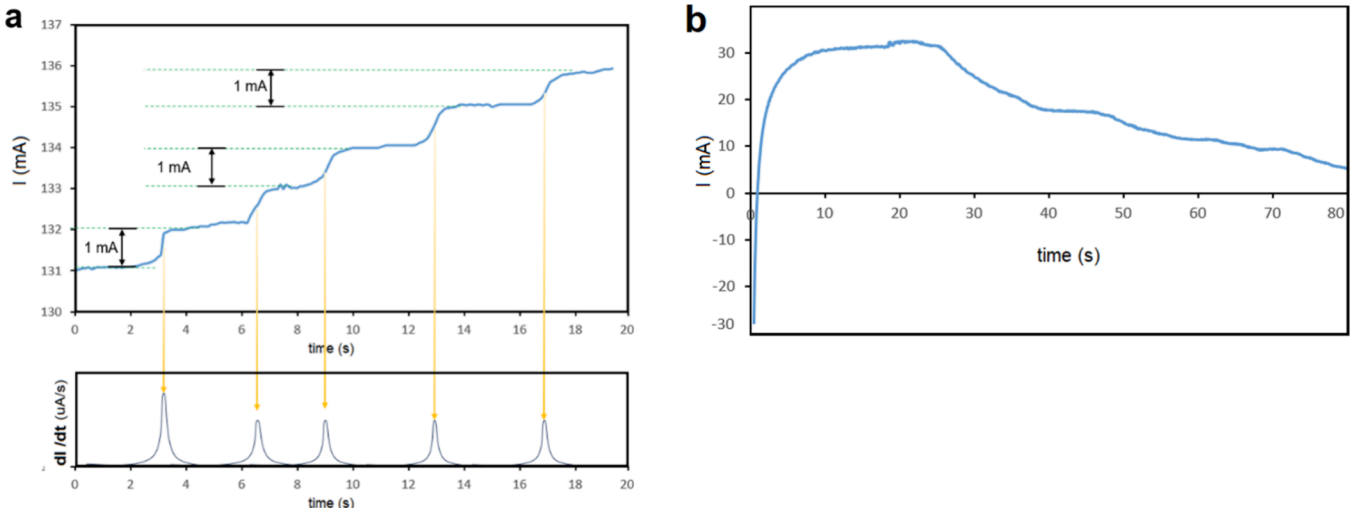

Figure 4. (a) Current steps that occurred during AgNP electrodeposition using 0.833 mM $AgNO_3$ as the Ag^+ precursor in this case. The augmented graph below was differential current showing the stepping time stamps. (b) 5 mM $AgNO_3$ at −0.5 V applied potential.

at 2 mM and diluted in DI. Reduction of gold ions (Au^{3+}) can be written as $AuCl^{4-} + 3e^- \rightarrow Au$ that occurred on the surface of GF. AuNPs/GF are characterized by FE-SEM in Figure 2. Electrochemical deposition current was plotted vs time in amperometric mode (Figures 3 and 4).

https://doi.org/10.1021/acsomega.4c01329
ACS Omega 2024, 9, 19591−19600

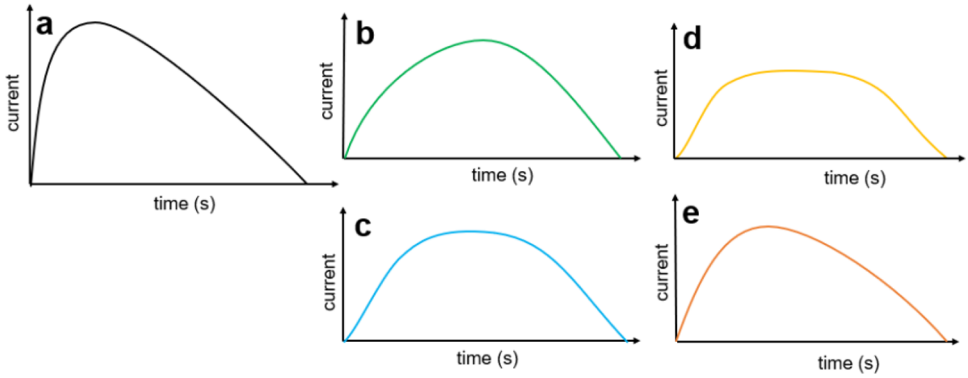

Figure 5. AuNP electrodeposition current (using 2 mM AuNPs) on flat graphene with a Si substrate using various applied potentials: (a) −0.5 V, (b) −0.4 V, (c) −0.3 V, (d) −0.2 V, and (e) −0.1 V. The current happens to be continuous. The vertical axis is normalized and plotted in arbitrary units.

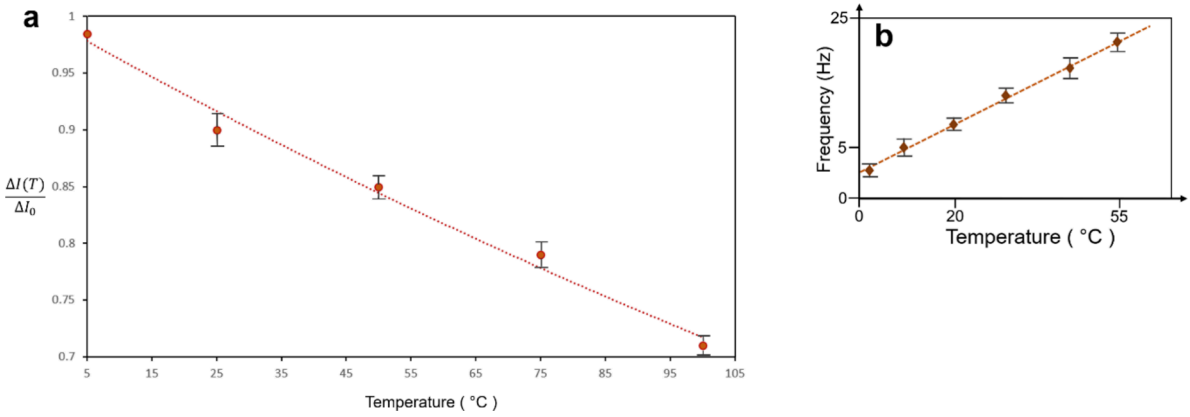

Figure 6. Temperature dependence plots: (a) current step size ratios vs temperature and (b) current transition frequency vs temperature.

2.3. Silver Electrodeposition onto GF. To check whether the step current could occur in other noble metal depositions, silver nanoparticles (AgNPs) were picked to test their properties. We chose silver since AgNPs have widespread usage from antibacterial to plasmonic materials.[9] Ag^+ ions were supplied by $AgNO_3$ dissolved in DI at different concentrations. In the experiment, we fixed the applied potential (for each round) and recorded the current versus time during the electrodeposition of Ag^+ ions onto GF, forming AgNPs on the surface of GF. We sought the potential that current steps might occur, starting with the potential used in the Au^{3+} case, and then we varied and repeated the amperometric deposition to determine the step size or to decide whether it is continuous.

2.4. Characterization. The deposited AuNP/GF was characterized by field-emission scanning electron microscopy (FE-SEM) as shown in Figure 2. The average size of AuNP was equal to 45 nm for both continuous and stepwise current cases. High-resolution tunneling electron microscopy (HR-TEM) was used to characterize and prove the presence of a graphene layer (Figure 2e).

3. RESULTS

The uniform current steps were recorded under specific electrochemical conditions without an externally applied magnetic field in a dirty electrochemical system at room temperature. The steps appeared during both AuNP and AgNP electrodepositions onto GF. The result was confirmed by repeating 100 pieces of GF growth under the same conditions. The temperature, applied magnetic field, and surface area dependencies are also reported. During the steps, the transition time increased over time. We name it "blocking time" due to the origin of this phenomenon, which will be discussed later on.

3.1. Uniform Current Steps and Blocking Time during Gold Nanoparticle Deposition. We divided electrodeposition into two parts: (i) AuNP and (ii) AgNP depositions. For each case, we varied the deposition potential ranging from −0.1 to −0.5 V. It was observed that stepwise deposition current occurred at -0.2 ± 0.1 V applied potential; otherwise, current would be continuous. The current step size was 1 mA for AgNP deposition and 1 μA for AuNP deposition.

The size of the step current remains uniform in both cases of increasing and decreasing stages of the current. The points in the time series where current steps occurred are shown in Figure 3c,e, where differential current was mapped with normal current. In AuNP deposition, the current step size was 1 μA at a −0.2 V potential and was continuous otherwise. Figure 3a exhibits deposition current in the continuous case, while Figure 3b−d shows the uniform current steps during electrodeposition. In another experiment, the behavior was repeated in silver deposition into graphene microporous. The current steps in silver deposition were on a larger scale at about 1 mA, and equal current step sizes occurred during the rising and lowering current stages for each material. The blocking time increases linearly as the deposition time increases (Figure 3f).

3.2. Uniform Current Step in Silver Nanoparticle Electrodeposition. Further investigation was carried out to determine whether the current steps could occur with other

https://doi.org/10.1021/acsomega.4c01329
ACS Omega 2024, 9, 19591−19600

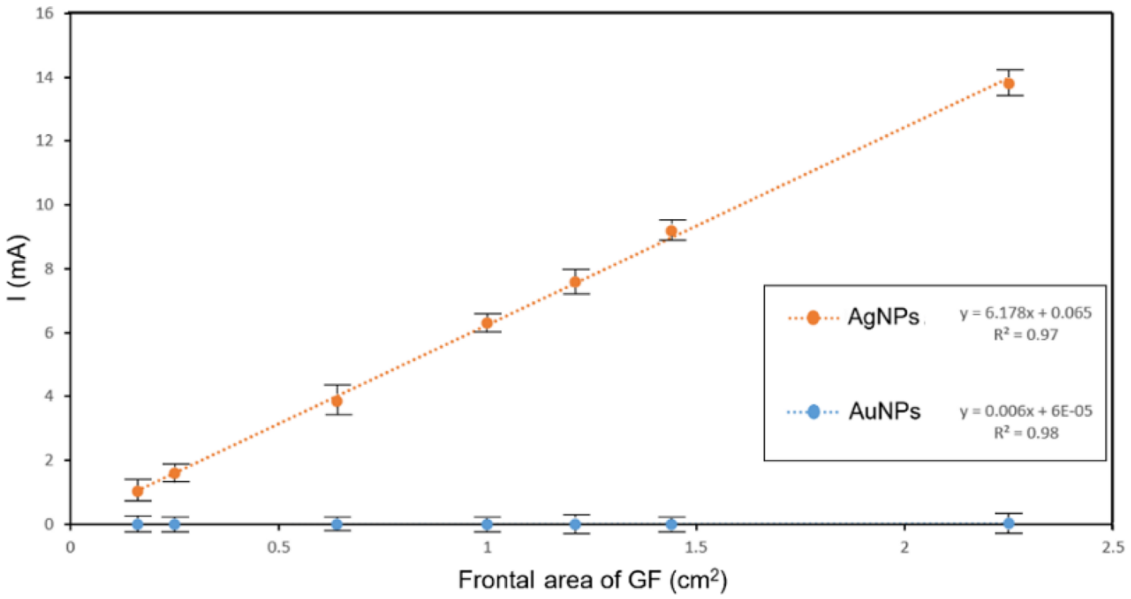

Figure 7. Current steps' amplitude and its GF-electrode area dependence: current step size plot vs frontal surface area of GF/Ni for AuNP and AgNP electrodepositions.

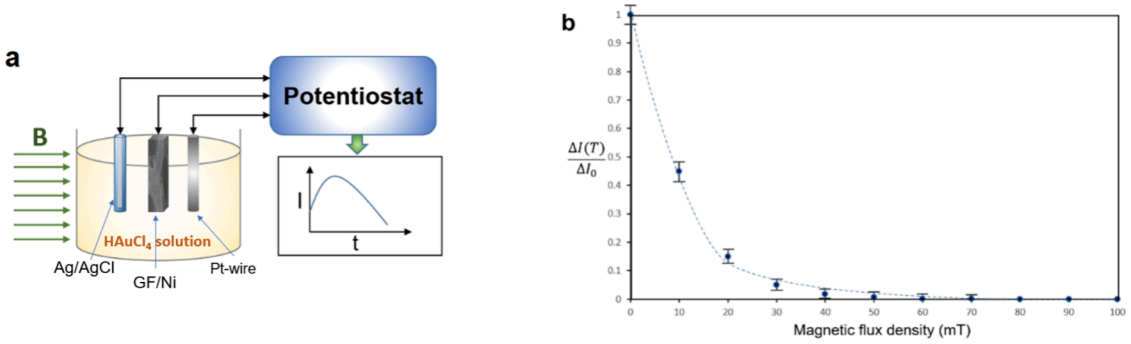

Figure 8. Interference by a magnetic field. (a) Experimental setup and (b) current step size vs magnetic flux interference plot. For each recorded experiment, the magnetic flux density was varied from 10, 20, 30, ..., 100 mT.

metallic nanoparticle growth. Silver nanoparticle (AgNP) electrodeposition on GF has shown a similar effect. $AgNO_3$ was used as the supply for Ag^+ ions to be reduced onto the GF surface. Changing the potential to −0.1, −0.3, −0.4, and −0.5 V results in continuous current. However, at −0.2 V applied potential, stepwise current occurred as shown in Figure 4a under various concentrations of Ag^+ of 0.833, 1.25, and 5 mM $AgNO_3$. In both rising and decreasing cases, the step sizes were equal, as illustrated as green dashed lines in Figure 4a. For other applied potentials, such as −0.5 V, the current curve appeared to be continuous, as can be seen in Figure 4b. Under various $AgNO_3$ concentrations, the stepwise current behavior still appears (Figure 4a).

3.3. Investigation on Flat Graphene. We investigated further whether this effect could be found in flat graphene. The experiments on various conditions have shown no step current (Figure 5). On the other hand, electrodeposition on 3D GF could yield current steps, as reported in the previous sections. An explanation will be in Section 5.

3.4. Temperature Dependence. We controlled the gold electrodeposition temperature from 5 to 100 °C and recorded the stepwise current. Experiments were repeated for 20 variations of different temperatures with 5 repetitions for each temperature condition. As the temperature increases, the step size decreases linearly. In addition, the current transition frequency between steps varies with temperature, as illustrated in Figure 6b.

3.5. Surface Area Dependence. We varied the size of the GF electrode and recorded the response current in which uniform current steps occurred. The plot between the graphene foam size and the corresponding current step size is added to Figure 7. The reactive surface area is proportional to the frontal area of GF/Ni piece. This result corresponds to the Butler−Volmer equation of faradaic current density, which will be mentioned in the classical theory section.

3.6. Magnetic Interference. We imposed a magnetic field to test its interference on the stepwise current behavior (Figure 8a). Current step ratios are plotted against the magnetic flux density in Figure 8b. The current steps began to diminish at 40−50 mT magnetic interference, where the current became continuous. This test was performed on gold nanoparticle deposition.

4. THEORY/CALCULATION

4.1. Classical Theory: Cyclotron Orbital Energy. We assume that electron modes are confined by a magnetic field (B) from the underlying nickel layer. The direction of the field induces a circular motion of electrons, as illustrated in Figure 9.

https://doi.org/10.1021/acsomega.4c01329
ACS Omega 2024, 9, 19591−19600

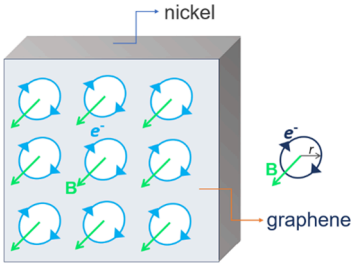

Figure 9. Electron charges are trapped in circular motion caused by a magnetic field (B) from the nickel layer, where r is the cyclotron radius.

According to cyclotron theory,[10] the energy of cyclotron orbits can be calculated as follows:

$$E = \frac{1}{2}mv^2 = \frac{(eBr)^2}{2m} \tag{1}$$

and cyclotron frequency is

$$\omega = \frac{v}{r} = \frac{eB}{m} \tag{2}$$

where v is the velocity, B is the magnetic flux density, r is the cyclotron radius, e is the charge of an electron, and m is the mass of the electron. The energy is then expressed as

$$E_N = NE = \frac{N(eBr)^2}{2m} \tag{3}$$

where N is the number of electrons circulating due to the magnetic field. These electrons were trapped and could not move freely. Therefore, an amount of energy is needed to remove those electrons from the graphene surface in a 3D structure (foam). Assuming that all electrons are in phase due to cyclotron spin coupling to the nearest neighboring sites, all of them should be removed at the same time. Hence, this results in a step current where fixed applied electric potential energy is matched to cyclotron energy, as in eq 3.

4.2. Classical Theory: Electrochemical. The electrochemical reaction rate can be described classically by the Butler–Volmer equation, i.e.,

$$\begin{aligned} j &= j_0 \cdot e^{[(\alpha_a zF/RT)(E-E_{eq})]} - e^{[(-\alpha_c zF/RT)(E-E_{eq})]} \\ &= j_a\{1 - e^{-\gamma(2\alpha_c-1)(E-E_{eq})}\} \end{aligned} \tag{4}$$

where $j_a = j_0 e^{\alpha_a \gamma(E-E_{eq})}$, $\gamma = \frac{zF}{RT}$, j is the current density at the electrode (A/m^2), j_0 is the exchange rate (A/m^2), E is the electrode potential (V), E_{eq} is the equilibrium potential (V), T is the absolute temperature (K), z is the number of electrons involved in the reaction, F is the Faraday constant, and R is the universal gas constant. α_a and α_c are anodic and cathodic charge transfer coefficients, respectively, where $\alpha_a + \alpha_c = 1$.

If $E - E_{eq}$ is constant, then $\frac{dj}{dt} = 0$, i.e., the current density j will be constant. However, if $E - E_{eq} = \Delta E$ is equal to the multiple number (N) of cyclotron energy (E_0), where $\Delta E = NE_0$, then j could jump with step E_0. We will consider the case where ΔE is matched to the cyclotron orbit of the electron in graphene and

$$\Delta E = NeV \tag{5}$$

for cyclotron electron energy potential. The jump in current will be

$$\Delta I = A\Delta j = \frac{Aj_a 2F}{RT}\Delta E = \frac{ANeF}{RT}V = \frac{1}{\eta R_K}V \tag{6}$$

where I denotes the current, A is the reactive area, $\eta = \frac{RT}{ANeFR_K}$, and $R_K = \frac{h}{e^2} \approx 25.8\ \text{k}\Omega$ is the von Klitzing constant.[11]

4.3. Quantum-Mechanical Explanation. In Landau quantization of cyclotron orbits, the corresponding energy can be expressed as[12]

$$E_N = \hbar\omega_c\left(N + \frac{1}{2}\right) + \frac{p_z^2}{2m} \tag{7}$$

where the cyclotron frequency ω_c is expressed by

$$\omega_c = \frac{eB}{m} \tag{8}$$

Note that electrons in graphene are confined to two dimensions. Therefore, the component $p_z = 0$ and the energy is thus

$$E_N = \frac{\hbar eB}{m}\left(N + \frac{1}{2}\right) \tag{9}$$

According to Landauer formalism, the current is given by

$$I = \frac{g_s e}{h}\int M(E)f'(E)T(E)\mathrm{d}E \tag{10}$$

where the spin g-factor $g_s = 2$, which comes from the Dirac equation, and $M(E)$ is the number of modes. $f(E)$ is the Fermi–Dirac distribution at room temperature, and $f'(E) = \mathrm{d}f/\mathrm{d}E$. N denotes the number of orbits, which are binding sites for metal ion deposition in our electrochemical reaction surface, and $T(E)$ is the transmission probability. An electron could transmit with the highest probability when the applied electric potential energy is equal to the total cyclotron energy of the electron. Therefore, the electric potential energy is $E_c = \Delta E = eV$, where E_c denotes the cyclotron energy.

Thus,

$$I = N\cdot\frac{2e}{h}T(E)f'(E)\Delta E \tag{11}$$

At certain potential, $M(E) = 1$ and the transmission probability $T(E)$ is equal to τ. The current is thus

$$I = \frac{2e}{h}f'(E)\Delta E\cdot\tau \tag{12}$$

At room temperature, $f'(E)$ could be considered as constant (please see Section 4.4).

Since

$$\Delta E = eV = N\hbar\omega_c = \frac{N\hbar eB}{m} \tag{13}$$

the current step thus occurs at $V = \frac{N\hbar B}{m}$.

$$\Delta I = \frac{2NBe^2}{m}f'(E)\cdot\tau \tag{14}$$

note that $R_K = \frac{h}{e^2} \approx 25.8\ \text{k}\Omega$ is the von Klitzing constant.[11]

Now, we write

https://doi.org/10.1021/acsomega.4c01329
ACS Omega 2024, 9, 19591−19600

$$\Delta I = \frac{4\pi V}{R_K} f'(E)\cdot\tau = \frac{f(E)\tau}{kT}\cdot\frac{4\pi}{R_K}V \tag{15}$$

or

$$\Delta I = \frac{V}{\eta R_K} \tag{16}$$

where V is the applied potential, and $\eta = kT/(4\pi f(E)\cdot\tau)$, which is defined as the von Klitzing ratio for the case of Au or Ag electron transfer, which was consistent with the experiments. The resistance term for Au and Ag electron transfer could be written as

$$R_{Au} = \eta_{Au} R_K \text{and} \eta_{Au} = 7.752 \tag{17}$$

$$R_{Ag} = \eta_{Ag} R_K \text{and} \eta_{Ag} = 7.752 \times 10^3 \tag{18}$$

where η_{Au} and η_{Ag} are the von Klitzing ratios of gold and silver that fit the experimental result. The current step size can be computed for gold and silver electrodepositions (eq 16).

The measured current step sizes in gold and silver electrodepositions were 1 μA and 1 mA, respectively. The energy differences in step size between metallic ions used could also be described by the transmission probability relation $T \propto e^{-2\beta d}$, where β is proportional to $(E - E_F^{Au})$ and $(E - E_F^{Ag})$, where E is the energy and E_F is the Fermi energy of gold and silver. Therefore, the difference in exponential terms attributed to different materials used for deposition (Au and Ag) would result in differences in experimental current step size, which were computed in eq 16.

4.4. Temperature Dependence. Fermi–Dirac distributions with different temperatures are plotted in Figure 10. At the Fermi energy (E_F) of GF, $f'(E)$ decreases as the temperature increases.

$$f(E) = \frac{1}{1 + e^{(E-E_F)/kT}} \approx e^{\frac{-(E-E_F)}{kT}} \tag{19}$$

$$f'(E) \approx \frac{1}{kT} f(E) \tag{20}$$

Therefore, the current step changes over increasing temperature can be computed using eqs 6 and 15 by

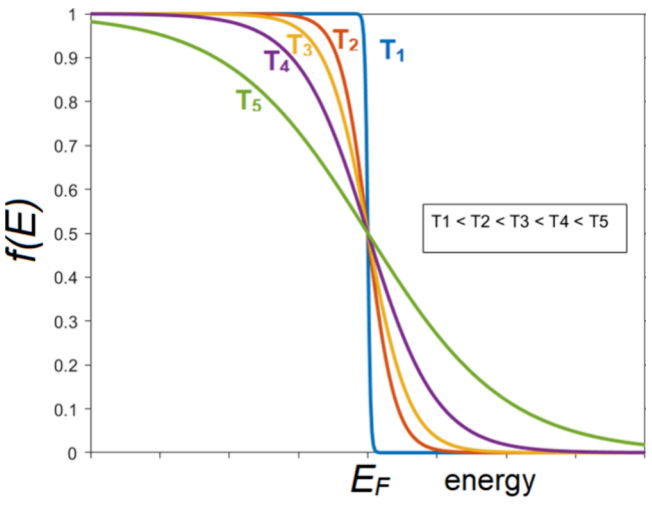

Figure 10. Fermi–Dirac distribution: energy vs $f(E)$ was plotted. The higher the temperature, the lower the slope of $f(E)$.

$$\frac{\Delta I(T_1)}{\Delta I(T_2)} = \frac{f'(E_F, T_1)}{f'(E_F, T_2)} = \frac{kT_2}{kT_1} = \frac{T_2}{T_1} \tag{21}$$

Let T_0 be the room temperature and T be an arbitrary increasing temperature. In our experiments, we heated the solutions using a hot plate. Therefore, the current step ratio would be

$$\frac{\Delta I(T)}{\Delta I(T_0)} = \frac{T_0}{T} = \frac{5 + 273.15}{T} \tag{22}$$

Both classical and quantum explanations predict (eqs 6 and 15) that the current step would decrease as the temperature increased, which agreed with the experiments.

4.5. Relation of Blocking Time vs Deposition Time. This section will derive why the blocking time t_{block} (Figure 1c,d) was a linear function of the deposition time t. Assume that each current step is to charge the capacitor with the amount of charge ΔQ and capacitance C at voltage V. Therefore, the current $\Delta I = \frac{\Delta Q}{t_{block}} = \frac{CV}{t_{block}}$, and the blocking time is thus

$$t_{block} = \frac{CV}{\Delta I} = C\eta R_K \tag{23}$$

where $C = \varepsilon A/d$, ε is the dielectric constant of the material, A is the surface area of the capacitor, and d is the distance of the charging surface. Now considering its time derivative, $\frac{dt_{block}}{dt} = \eta R_K \frac{dC}{dt} = \eta R_K \frac{d(\varepsilon A/d)}{dt} = \frac{\eta R_K A}{d}\cdot\frac{d\varepsilon}{dt}$, where A and d were fixed, we will find the solution whether it is positive or negative. According to the Drude model,[13] the dielectric constant is

$$\varepsilon = 1 - \frac{Ne^2}{\varepsilon_0 m\omega_c^2} \tag{24}$$

its derivative over time will be

$$\frac{d\varepsilon}{dt} = -\frac{Ne^2}{\varepsilon_0 m\omega_2^c}\cdot\frac{dN}{dt} = c = \text{constant} \tag{25}$$

c is a nonnegative constant since $dN/dt \sim$ negative. Therefore, $t_{block} = \frac{\eta R_K A}{d}\int c\,dt = \frac{\eta R_K A c}{d} t$, which is positively proportional to the deposition time t. As the deposition time (t) increased, more nanoparticles were deposited to GF and the GF's available surface for cyclotron orbits would be reduced (Figure 11). t_{block} thus increases proportionally over time corresponding to the reduction of deposition rate ($dN/dt \sim$ negative).

5. DISCUSSION

The stepwise current behavior appeared in both gold and silver electrodepositions on graphene/nickel foam under certain conditions, mainly depending on the applied potential. The differences between steps are equal for both the raising and lowering stages of the deposition current. The current step (ΔI) can be calculated using cyclotron orbits where electrons are assumed to move circularly due to the magnetic field from very close proximity of the nickel substrate. In addition, the current step can also be computed by using classical theory and quantum theory. Both theories are consistent with the experimental results. For temperature factors, it showed that the step diminishes at high temperatures. The influence of

https://doi.org/10.1021/acsomega.4c01329
ACS Omega 2024, 9, 19591–19600

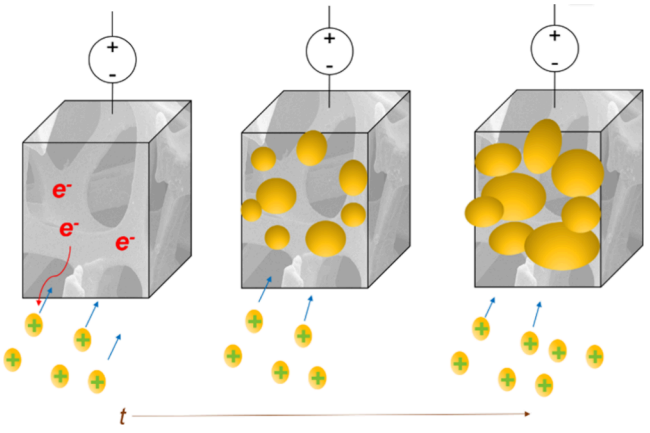

Figure 11. The available reactive area decreases as time increases. This results in the increment in the blocking time (transition time between the sharp steps).

temperature on current could be explained by Fermi–Dirac statistics and the Faradaic term in classical theory.

In AuNP electrodeposition on GF, we compared the nanoparticle size distribution between the continuous and stepwise deposition currents. The size distribution and morphology of the nanoparticles could not be noticed between the cases of continuous and stepwise currents, as the diameters for both cases are plotted in Figure 2d.

The surface area dependencies on the current step size can be explained by classical theory, the Butler–Volmer equation. The increase in the blocking time (Figure 1c,d) could be derived from the Drude model, as in the previous section. The step size could be computed from Landauer formalism.

The steps could not be noticed in 2D graphene experiments because the current step size is proportional to the reactive surface area (Butler–Volmer). Since 2D graphene has a much lower (10^{-4}) surface area per unit volume compared to 3D microporous graphene,[14] the current steps that could occur in 2D graphene would be too small and unnoticeable.

As the temperature increases, the current step size decreases. The step amplitudes versus temperature are plotted in Figure 6a. The experimental results correspond well with eqs 6 and 15, implying that the current step size is proportional to the slope of $f(E)$ at the Fermi energy level of graphene and Faradaic constant term, which is inversely proportional to temperature in eq 6.

The external magnetic field significantly influences the occurrence of steps. The applied magnetic field could disturb the global anisotropic but internal isotropic magnetic field from the 3D nickel/graphene scaffold. The steps disappear at magnetic fields >50 mT (Figures 8 and 12). The local magnetic fields from Ni foam scaffolds, oriented uniformly orthogonal to its local surface, induce electron cyclotron motion. In this scenario, electrons move coherently because of spin coupling between neighboring orbits (Figure 9). The external magnetic field would disturb electrons to display decoherence in movement, preventing them from being part of the entire coherent cyclotron bundle, resulting in a smaller number of cyclotron orbitals as the external magnetic field increases and hence decreases the step current where $\Delta I \propto N$ (N is denoted as the number of cyclotron orbits).

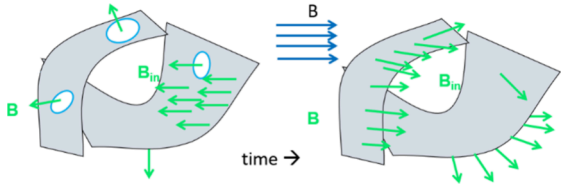

Figure 12. The external magnetic field induced all magnetic fields to change. The local magnetic field was previously moving coherently, like a cyclotron.

The accumulated charge (Q) can be related to the temperature, surface area, blocking effect, and magnetic field influence as follows: The accumulated charge is $Q(t) = Q(t_0) + \Delta Q$, where $Q(t_0) = \int I(t_0)dt$ is the accumulated charge at time t_0 and $\Delta Q = \Delta I \cdot t_{block}$, i.e., the charge accumulation amount is proportional to the current step size times the (increasing) blocking time (t_{block}). According to eq 22, $\frac{\Delta I(T)}{\Delta I(T_0)} = \frac{T_0}{T} = \frac{5 + 273.15}{T}$, the temperature is inversely proportional to ΔI and ΔQ. Q plotted as a function of temperature, surface area, blocking time, and applied magnetic field is shown in Figure 13. The sizes of GF were varied to plot Q versus reactive area (A). The experimental results (Figure 13c) fit $Q = CV = \varepsilon A/d$.

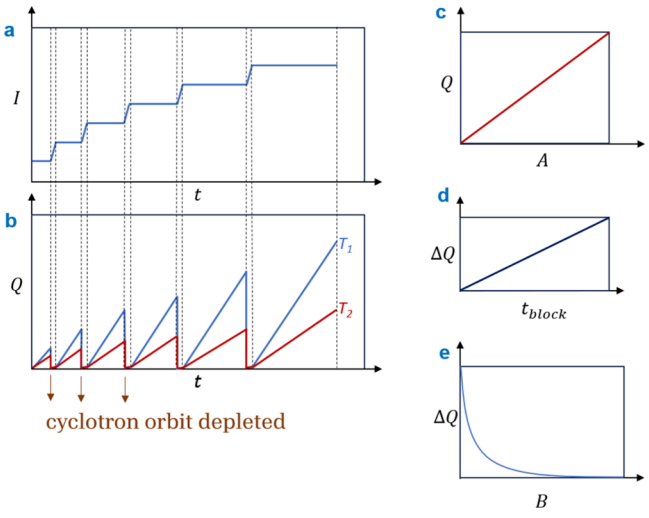

Figure 13. Accumulated charge (Q) plotted over time with various conditions: (i) different temperatures, (ii) varying surface area, (iii) blocking time, and (iv) applied magnetic field intensity. (a) Recap of step current observed. (b) Q over time under different temperatures $T_1 < T_2$. (c, d) Reactive area (A) and t_{block} linearly relate to Q or ΔQ. (e) Q decreases exponentially and approaches zero as the applied magnetic field strength increases.

The reason the current step size of two metals differs is due to the difference between the transmission distances of the dielectric bilayer of metal ions in the electrolyte solution. Normally, $T(E) \propto \exp(-d_M)$ where M can be Au or Ag in this study (Figure 14). Another reason is that there will be a diffusion rate between two metals since, according to Fick's law, $J = D\frac{dN}{dx} \approx \frac{DN}{d_M}$, where D is the diffusion coefficient in the solution. As the thickness increases, the current density decreases. Therefore, different dielectric bilayer thicknesses will result in different current densities and different current steps for gold and silver.

To investigate the possibility of a hydrogen bubble detachment mechanism during deposition,[15] we have carried

https://doi.org/10.1021/acsomega.4c01329
ACS Omega 2024, 9, 19591–19600

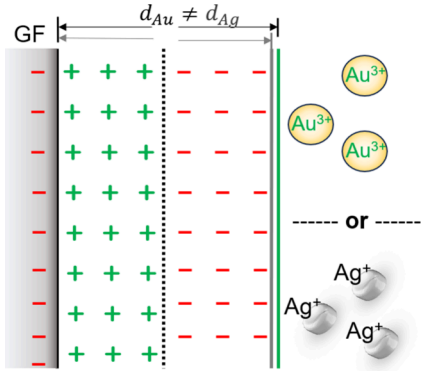

Figure 14. Dielectric bilayer thicknesses (d_{Au} and d_{Ag}) are not equal for the two cases: GF and gold ions (Au^{3+}); GF and silver ions (Ag^{+}).

out experiments under varying magnetic stirring speeds (400, 500, 600, and 700 rpm). The results were reproduced, and 400 rpm was used for the rest of the depositions. The current step size remains constant. If the effects were caused by the hydrogen bubbles, then they should have occurred at every potential applied to the electrodes, which is not the case in the experimental results. Since hydrogen bubbling is a stochastic process, the step size should not be equal at all for any conditions. In the experiment, we observed an anomalous step current at a specific potential. Therefore, we could exclude the case of bubble attachment.

The discussion can be summarized as follows:

- Both quantum and classical theories are consistent, and the combination of them could describe the results.
- The current step size in the Landau equation is equal to that computed from Landauer formalism and agrees with the experiment.
- The Landauer formulation concludes that the current step size should be equal for each material. This is consistent with the results.
- A limitation of using the Landau equation is that they could not describe surface area dependencies on the current step size. Meanwhile, the classical theory using the Butler–Volmer equation could explain that the size of step current is proportional to the surface area.
- The current can be written in Ohm's law analogy, where resistance is a deposited material-specific constant multiplied by the von Klitzing constant and metal type-specific coefficients (eqs 16–18).
- Increasing the external magnetic field can disrupt the internally uniform magnetic field of the local site in the graphene/nickel layer. This external field causes the cyclotron orbits to display decoherence, leading to a smaller step size.
- The blocking time linearly increases with the deposition time, and this could be explained in the Drude model.
- Classical theory could also describe the inversely proportional relation between temperature and step size using Fermi–Dirac statistics (eqs 19 and 21).
- We have not varied the pore size of GF because we fabricated it using a Ni foam scaffold as the catalyst. An investigation on how pore size affects the resulting stepwise current can be further investigated in another work.
- The Pt electrode used as the counter electrode could probably yield current contamination. Therefore, we repeated the experiment by replacing the Pt electrode with a graphite rod, and the step current behavior was still reproduced.

6. CONCLUSIONS

We reported uniform current step behavior in an electrochemical system using a 3D microporous graphene/nickel electrode, with equal current steps consistently recorded during repetitions of gold and silver electrodepositions. Both classical and quantum theories were formulated to explain this phenomenon. The current step sizes for Ag and Au electrodepositions were calculated using our derivation from the Landau and Landauer formalism (eqs 16–18), which agree with the experiments. The classical and quantum cyclotron models, which explain electrons as being confined in cyclotron orbits, could describe temperature dependencies, magnetic dependencies, and blocking time. Faradaic coefficient Fermi–Dirac statistics could explain temperature dependence on the current steps. This suggests the potential of using electrons confined on graphene surfaces as cyclotrons to release a large amount of current in a very short transition time.

A. APPENDIX

A.1. Supporting Videos

Experimental videos showing the step current during electrodeposition can be found in the following links:

1. During gold electrodeposition into GF (link to video: https://youtu.be/pPJh45w1sUQ).
2. During gold electrodeposition into GF. Electrode contact was human-disturbed, yielding spikes at the middle of the graph. Afterward, the uniform current step observation continues (link to video: https://youtu.be/Axi0AWvA0V0).

ASSOCIATED CONTENT

Data Availability Statement

All underlying data available in the article itself.

AUTHOR INFORMATION

Corresponding Author

Chavis Srichan − *Faculty of Engineering, Khon Kaen University, Khon Kaen 40002, Thailand;* orcid.org/0000-0002-4772-3543; Email: chavis@kku.ac.th

Authors

Pobporn Danvirutai − *Faculty of Engineering, Khon Kaen University, Khon Kaen 40002, Thailand*

Adisorn Tuantranont − *Graphene and Printed Electronics for Dual-Use Application (GPERD), National Science and Technology Development Agency, Pathum Thani 12120, Thailand*

Complete contact information is available at: https://pubs.acs.org/10.1021/acsomega.4c01329

Author Contributions

C.S.: conceptualization, methodology, investigation, formal analysis, and writing of the original draft. P.D.: methodology, investigation, visualization, and validation. A.T.: resources, supervision, project administration, and review and editing.

Notes

The authors declare no competing financial interest.

https://doi.org/10.1021/acsomega.4c01329
ACS Omega 2024, 9, 19591−19600

■ ACKNOWLEDGMENTS

We would like to gratefully acknowledge collaboration with the Biomedical Engineering Department, Mahidol University, especially Dr. Manop Sansuk, and the warm memories of Prof. Pornpimol Sritongkham. We greatly appreciate the facilities supported by the Department of Chemistry, KKU, via Assoc. Prof. Pittayakorn Noisong and Dr. Saifon Kullyakool (NSTDA). C.S. and P.D. are deeply grateful to Asst. Prof. Chanchai Vithsupalert for his invaluable lectures.

■ REFERENCES

(1) Chen, Z.; Ren, W.; Gao, L.; Liu, B.; Pei, S.; Cheng, H.-M. Three-Dimensional Flexible and Conductive Interconnected Graphene Networks Grown by Chemical Vapour Deposition. *Nat. Mater.* **2011**, *10*, 424−428.

(2) Zhao, Y.; Liu, J.; Hu, Y.; Cheng, H.; Hu, C.; Jiang, C.; Jiang, L.; Cao, A.; Qu, L. Highly Compression-Tolerant Supercapacitor Based on Polypyrrole-Mediated Graphene Foam Electrodes. *Adv. Mater.* **2013**, *25*, 591−595.

(3) Xu, S.; Zhang, C.; Jiang, S.; et al. Graphene Foam Field-Effect Transistor for Ultra-Sensitive Label-Free Detection of ATP. *Sens. Actuators B Chem.* **2019**, *284*, 125−133.

(4) Danvirutai, P.; Ekpanyapong, M.; Tuantranont, A.; Bohez, E.; Anutrakulchai, S.; Wisitsoraat, A.; Srichan, C. Ultra-Sensitive and Label-Free Neutrophil Gelatinase-Associated Lipocalin Electrochemical Sensor Using Gold Nanoparticles Decorated 3D Graphene Foam Towards Acute Kidney Injury Detection. *Sens. Bio-Sens. Res.* **2020**, *30*, No. 100380.

(5) Wang, X.; Guo, X.; Chen, J.; Ge, C.; Zhang, H.; Liu, Y.; Zhao, L.; Zhang, Y.; Wang, Z.; Sun, L. Au Nanoparticles Decorated Graphene/Nickel Foam Nanocomposite for Sensitive Detection of Hydrogen Peroxide. *J. Mater. Sci. Technol.* **2017**, *33*, 246−250.

(6) Srichan, C.; Ekpanyapong, M.; Horprathum, M.; Eiamchai, P.; Nuntawong, N.; Phokharatkul, D.; Danvirutai, P.; Bohez, E.; Wisitsoraat, A.; Tuantranont, A. Highly-Sensitive Surface-Enhanced Raman Spectroscopy (SERS)-Based Chemical Sensor Using 3D Graphene Foam Decorated with Silver Nanoparticles as SERS Substrate. *Sci. Rep.* **2016**, *6*, 23733.

(7) Xu, Y.; Yang, C.; Wang, M.; Pan, X.; Zhang, C.; Liu, M.; Xu, S.; Jiang, S.; Man, B. Adsorbable and Self-Supported 3D AgNPs/G@Ni Foam as Cut-and-Paste Highly-Sensitive SERS Substrates for Rapid In Situ Detection of Residuum. *Opt. Express* **2017**, *25*, 16437−16451.

(8) Novoselov, K. S.; Morozov, S. V.; Mohinddin, T. M. G.; et al. Electronic Properties of Graphene. *Phys. Status Solidi (b)* **2007**, *244*, 4106−4111.

(9) Lim, Y. H.; Tiemann, K. M.; Heo, G. S.; Wagers, P. O.; Rezenom, Y. H.; Zhang, S.; Zhang, F.; Youngs, W. J.; Hunstad, D. A.; Wooley, K. L. Preparation and In Vitro Antimicrobial Activity of Silver-Bearing Degradable Polymeric Nanoparticles of Polyphosphoester-Block-Poly(l-lactide). *ACS Nano* **2015**, *9* (2), 1995−2008.

(10) Seidel, M. *Cyclotrons for High-Intensity Beams*, CERN, 2013. Available at https://cds.cern.ch/record/1513944/files/CERN-2013-001-p17.pdf (accessed 2022−06−12).

(11) Neto, A. C.; Peres, N. M. R.; Novoselov, K. S.; Geim, A. K. The Electronic Properties of Graphene. *Rev. Mod. Phys.* **2009**, *81* (1), 109−162.

(12) Landau, L. D.; Lifschitz, E. M. *Quantum Mechanics: Non-Relativistic Theory*, 3rd ed.; Pergamon Press, 1977; ISBN 0750635398.

(13) Fox, A. M. *Optical Properties of Solids*; Oxford University Press, 2001; ISBN 0198506120.

(14) Drieschner, S.; Weber, M.; Wohlketzetter, J.; Vieten, J.; Makrygiannis, E.; Blaschke, B. M.; Morandi, V.; Colombo, L.; Bonaccorso, F.; Garrido, J. A. High Surface Area Graphene Foams by Chemical Vapor Deposition. *2D Mater.* **2016**, *3*, No. 045013.

(15) Belotti, M.; El-Tahawy, M. M.; Garavelli, M.; Coote, M. L.; Iyer, K. S.; Ciampi, S. Separating Convective from Diffusive Mass Transport Mechanisms in Ionic Liquids by Redox Pro-fluorescence Microscopy. *Anal. Chem.* **2023**, *95* (26), 9779−9786.

https://doi.org/10.1021/acsomega.4c01329
ACS Omega 2024, 9, 19591−19600